Article

Mechanisms and Applications of Plasmon-Induced Charge Separation at TiO Films Loaded with Gold Nanoparticles

Yang Tian, and Tetsu Tatsuma

J. Am. Chem. Soc., **2005**, 127 (20), 7632-7637• DOI: 10.1021/ja042192u • Publication Date (Web): 29 April 2005

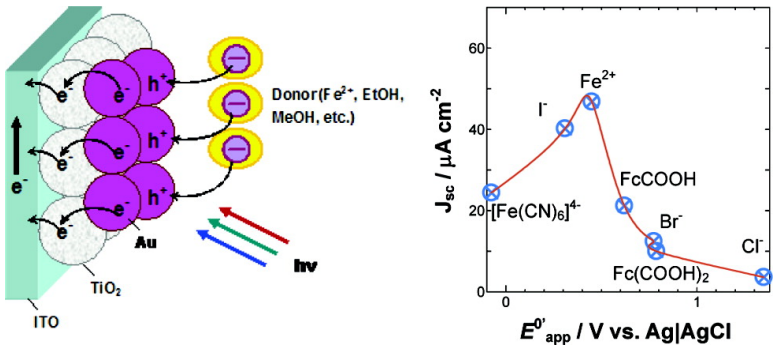

More About This Article

Additional resources and features associated with this article are available within the HTML version:

- Supporting Information
- Links to the 25 articles that cite this article, as of the time of this article download
- Access to high resolution figures
- Links to articles and content related to this article
- Copyright permission to reproduce figures and/or text from this article

View the Full Text HTML

J|A|C|S
ARTICLES
Published on Web 04/29/2005

Mechanisms and Applications of Plasmon-Induced Charge Separation at TiO_2 Films Loaded with Gold Nanoparticles

Yang Tian and Tetsu Tatsuma*

Contribution from the Institute of Industrial Science, The University of Tokyo, 4-6-1 Komaba, Meguro-ku, Tokyo 153-8505, Japan

Received December 28, 2004; E-mail: tatsuma@iis.u-tokyo.ac.jp

Abstract: Plasmon-induced photoelectrochemistry in the visible region was studied at gold nanoparticle−nanoporous TiO_2 composites (Au−TiO_2) prepared by photocatalytic deposition of gold in a porous TiO_2 film. Photoaction spectra for both the open-circuit potential and short-circuit current were in good agreement with the absorption spectrum of the gold nanoparticles in the TiO_2 film. The gold nanoparticles are photoexcited due to plasmon resonance, and charge separation is accomplished by the transfer of photoexcited electrons from the gold particle to the TiO_2 conduction band and the simultaneous transfer of compensative electrons from a donor in the solution to the gold particle. Besides its low-cost and facile preparation, a photovoltaic cell with the optimized electron mediator ($Fe^{2+/3+}$) exhibits an optimum incident photon to current conversion efficiency (IPCE) of 26%. The Au−TiO_2 can photocatalytically oxidize ethanol and methanol at the expense of oxygen reduction under visible light; it is potentially applicable to a new class of photocatalysts and photovoltaic fuel cells.

Introduction

Metal nanoparticles are of great interest because of their unique electronic, optical, and magnetic properties.[1−5] In particular, nanoparticles of noble metals such as gold and silver have been attracting more attention[6−8] because they have many color varieties in the visible region based on plasmon resonance, which is due to the collective oscillations of the electrons at the surface of the nanoparticles. The resonance wavelength strongly depends on the size and shape of the nanoparticles, the interparticle distance, and the dielectric property of the surrounding medium. The unique plasmon absorbance features of these noble metal nanoparticles have been exploited for a wide variety of applications[9] including chemical sensors and biosensors. Plasmon-induced photochemical reactions have also been employed to produce silver nanoprisms and gold nanorods.[7,8,10,11] Photoinduced "melting" of gold nanorods, which is likely based on nonradiative deactivation of the plasmon, has been exploited for irreversible writing of an image.[12] We have reported reversible photoinduced multicolor imaging (multicolor photochromism) of silver nanopaticles deposited in a nanoporous TiO_2 film by photocatalytic means.[13,14]

However, charge separation at a plasmon-excited metal nanoparticle without degradation (e.g., corrosion) of the particle has never been reported to the best of our knowledge. If this is possible, photovoltaic cells[15] with expensive organic dyes and inorganic dyes with organic ligands would be improved in terms of cost and stability. A new class of visible light-sensitive photocatalysts and photovoltaic fuel cells are additional potential applications. Although metal nanoparticles have been employed in photocatalysts[16] and photovoltaic cells,[17] the particles have not been used as photosensitizers.

Although Kozuka et al.[18] have observed anodic photocurrents in response to visible light irradiation at gold- and silver-deposited TiO_2 films, the stability of the metals is unknown. In addition, they had to apply a large bias voltage to obtain action spectra because they did not add an appropriate electron donor. Recently, we have reported photoelectrochemistry at gold and silver nanoparticles incorporated in nanoporous TiO_2.[19] We have developed almost, but not completely, stable systems by combining it with an electron donor (I^-) and demonstrated

(1) Murry, C. B.; Kagan, C. R.; Bawendi, M. G. *Science* **1995**, *270*, 1335−1338.
(2) Ziolo, R. F.; Giannelis, E. P.; Weinstein, B. A.; O'Horo, M. P.; Ganguly, B. N.; Mehrotra, V.; Russell, M. W.; Huffmann, D. R. *Science* **1992**, *257*, 219−223.
(3) Kang, Y. S.; Risbud, S.; Rabolt, J. F.; Stroeve, P. *Chem. Mater*. **1996**, *8*, 2209−2211.
(4) Collier, C. P.; Saykally, R. J.; Shiang, J. J.; Henrichs, S. E. H. J. R. *Science* **1997**, *277*, 1978−1981.
(5) Zhao, M.; Sun, L.; Crooks, R. M. *J. Am. Chem. Soc*. **1998**, *120*, 4877−4878.
(6) Link, S.; El-Sayed, M. A. *J. Phys. Chem. B* **1999**, *103*, 8410−8426.
(7) Jin, R.; Cao, Y. C.; Mirkin, C. A.; Kelly, K. L.; Schatzand, G. C.; Zheng, J. G. *Science* **2001**, *294*, 1901−1903.
(8) Mock, J. J.; Barbic, M.; Smith, D. R.; Schults, D. A.; Schults, S. *J. Chem. Phys*. **2002**, *116*, 6755−6759.
(9) Daniel, M.-C.; Astruc, D. *Chem. Rev*. **2004**, *104*, 293−346.
(10) Jin, R.; Cao, Y. C.; Hao, E.; Métrauz, G. S.; Schatz, G. C.; Mirkin, C. A. *Nature* **2003**, *425*, 487−490.
(11) Kim, F.; Song, J. H.; Yang, P. *J. Am. Chem. Soc*. **2002**, *124*, 14316−14317.
(12) Wilson, B. O.; Wilson, G. J.; Mulvaney, P. *Adv. Mater*. **2002**, *14*, 1000−1004.
(13) Ohko, Y.; Tatsuma, T.; Fujii, T.; Naoi, K.; Niwa, C.; Kubota, Y.; Fujishima, A. *Nature Mater*. **2003**, *2*, 29−31.
(14) Naoi, K.; Ohko, Y.; Tatsuma, T. *J. Am. Chem. Soc*. **2004**, *126*, 3664−3668.
(15) Grätzel, M. *Nature* **2001**, *414*, 338−344.
(16) Bard, A. J. *J. Phys. Chem*. **1982**, *86*, 172−177.
(17) Subramanian, V.; Wolf, E.; Kamat, P. V. *J. Phys. Chem. B* **2001**, *105*, 11439−11446.
(18) Zhao, G.; Kozuka, H.; Yoko, T. *Thin Solid Films* **1996**, *277*, 147−154.
(19) Tian, Y.; Tatsuma, T. *Chem. Commun*. **2004**, 1810−1811.

10.1021/ja042192u CCC: $30.25

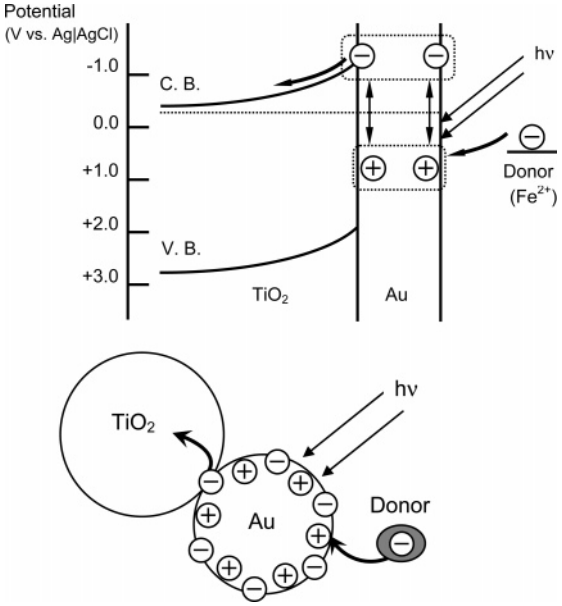

Figure 1. Proposed mechanism for the photoelectrochemistry. Charges are separated at a visible-light-irradiated gold nanoparticle−TiO_2 system.

complete matching between the plasmon absorption spectra of the metal nanoparticles and photopotential and photocurrent action spectra obtained without bias voltage. Thus we have verified that our system is potentially applicable to inexpensive photovoltaic cells and visible-light-sensitive photocatalysts.

However, the mechanism is still unknown, and as a photovoltaic cell, the incident photon to current conversion efficiency (IPCE) was too low (1% for Au−TiO_2) for practical applications. In the present work, we examined a series of donors for the Au−TiO_2 and the IPCE was improved by a factor of >20. Also, we found that the Au−TiO_2 is potentially applicable to visible-light-induced photocatalytic oxidation of ethanol and methanol and reduction of oxygen. In addition, we studied the mechanism of the system and evidenced that the photoelectrochemistry is based on the charge separation at the gold nanoparticles, which includes electron transfer from the plasmon-excited gold to TiO_2 and that from a donor to the gold (Figure 1).

Experimental Section

Chemicals and Materials. Acetonitrile (analytical grade), ethylene glycol (analytical grade), lithium nitrate, iron(II) chloride, potassium iodide, potassium chloride, ethanol (99.5%), and methanol (99.5%) were purchased from Wako Pure Chemical Industries, Ltd. (Osaka, Japan) and used as supplied. Iron(III) chloride, potassium bromide, and potassium ferrocyanide were purchased from Kanto Chemical Co., Inc. (Tokyo, Japan). Ferrocenecarboxylic acid and 1,1′-ferrocenedicarboxylic acid were obtained from Aldrich Chemical Co., Inc. and used without further purification. The solution used in this work was freshly prepared and deoxygenated by bubbling nitrogen gas for at least 30 min prior to use.

Preparations of TiO_2 and Au−TiO_2 Films. A TiO_2 film was prepared as follows: an ITO-coated glass plate was coated with a nanoporous TiO_2 film prepared from an anatase TiO_2 sol (Ishihara Sangyo Kaisha, STS-21, 20 nm particle diameter) by spin-coating (sintered at 723 K for 1 h). The film thickness was 4 μm. A thicker TiO_2 film (10 μm) employed in the measurements of total energy conversion efficiency was prepared from TiO_2 paste (Peccell Technologies, Japan) by the squeegee method and sintered at 423 K for 15 min. The former TiO_2 film was used unless otherwise noted. For the preparation of a Au−TiO_2 film, we employed a photocatalytic reduction method widely reported for the preparation of metal nanoparticles (e.g., Pt, Cu, Ag, Pd, and Au) on TiO_2 films.[13,14,20,21] A TiO_2 film was soaked in 5 mM aqueous $HAuCl_4$ for about 30 min and rinsed with water. Then, the film was irradiated with ultraviolet light (1 mW cm^{-2}) for at least 1 h to reduce the adsorbed Au^{3+} to Au by TiO_2 photocatalysis at the expense of water oxidation.

Instruments and Measurements. The UV absorption spectra of the films were measured using a UV spectrophotometer (UV-2400PC, Shimadzu, Japan). An HZ 3000 automatic polarization system (Hokuto Denko, Japan) was employed in electrochemical measurements. Photoaction spectra for the potential changes were obtained in a conventional two-compartment three-electrode electrochemical cell. The reference electrode was a KCl-saturated Ag|AgCl electrode, while the auxiliary electrode was a platinum wire. To test the performance of each electron donor, a platinum wire was employed as the counter electrode in a two-compartment two-electrode cell. On the other hand, action spectra for the photocurrent changes and energy conversion efficiency were obtained in a two-electrode sandwich cell (thickness of the electrolyte, 5 mm). The counter electrode was a gold film sputtered on an ITO-coated glass plate. The Au−TiO_2 substrate was irradiated with a white light (λ > 420 or 500 nm) using a xenon lamp with an ultraviolet-cutoff filter from the back. Action spectra were collected using a xenon lamp with an appropriate band-pass filter (fwhm, 10 nm) or a M25 monochromator (fwhm, 20 nm) (Bunkou Keiki, Japan). A Hitachi S-4500 (Japan) scanning electron microscope (SEM) was employed to record the images with 100 K magnifications. The structures of TiO_2 and Au−TiO_2 films were analyzed by X-ray photoelectron spectroscopy (XPS) using a Quantum-2000 Scanning ESCA microprobe (ULVAC-PHI, Inc.) with Mg Kα radiation.

Results and Discussion

Characterization of the Au−TiO_2 Film. The visible absorption spectrum of gold deposited in the nanoporous TiO_2 film was clearly characterized by the plasmon resonance peak of gold nanoparticles (Figure 2B, curve b). In comparison with commercially available gold nanoparticles (AuE-101, 5−20 nm diameter, Nippon Paint) suspended in ethanol (Figure 2B, curve a), the peak of the photocatalytically deposited one was red-shifted and broadened due to the high refractive index of anatase TiO_2 (2.52).[22] Another possible explanation might be formation of an indirect charge transfer band.[23] Incidentally, apparent absorption of the unmodified TiO_2 film in the visible region (Figure 2A) should be ascribed to light scattering, because the film was not visibly colored before the deposition of gold.

We verified that the deposited gold was metallic by X-ray photoelectron spectroscopy (XPS) (inset of Figure 2A). The peaks observed at 84.0 and 87.7 eV were ascribed to metallic gold. In addition, the diameter of the particles observed in SEM images of the present Au−TiO_2 film was less than 50 nm (inset of Figure 2B). Thus, we can conclude that nanosized gold particles are formed in the TiO_2 film. Also, XPS measurements combined with film etching proved that the gold nanoparticles were distributed in the whole film, although the particles were somewhat concentrated in the surface region.

Dependence of the Photovoltaic Performance on the Donor. As we have reported previously, the Au−TiO_2 can be

(20) Kraeutler, B.; Bard, A. J. *J. Am. Chem. Soc.* **1978**, *100*, 4317−4318.
(21) Subramanian, V.; Wolf, E. E.; Kamat, P. V. *Langmuir* **2003**, *19*, 469−474.
(22) Fujishima, A.; Hashimoto, K.; Watanabe, T. *TiO_2 photocatalysis*: *fundamentals and applications*; BKC: Tokyo, 1999; p 125.
(23) Yang, M.; Thompson, D. W.; Meyer, G. J. *Inorg. Chem.* **2002**, *41*, 1254−1262.

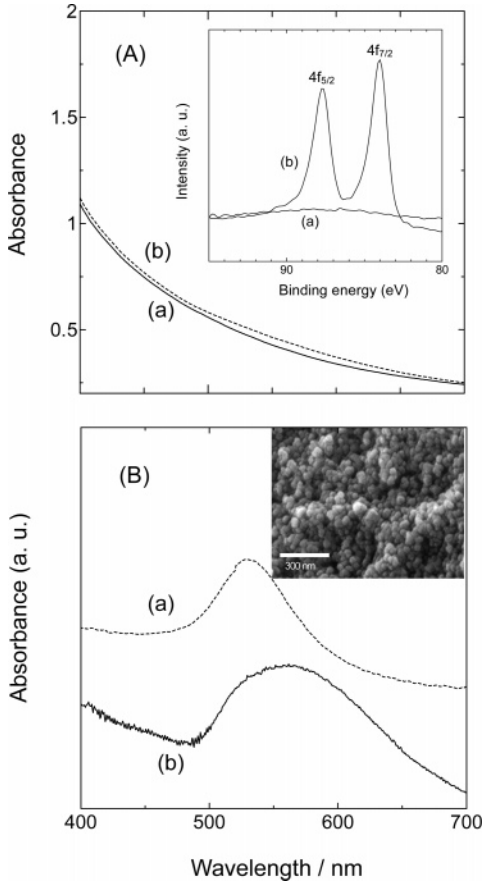

Figure 2. Absorption spectra of (A-a) the nanoporous TiO_2 film, (A-b) $Au-TiO_2$ film (gold nanoparticles were deposited by photocatalytical means), (B-a) commercially available gold nanoparticles suspended in ethanol, and (B-b) gold nanoparticles deposited photocatalytically in the TiO_2 film (the spectrum of TiO_2 has been subtracted). Inset in A: X-ray photoelectron spectra of the TiO_2 (a) and $Au-TiO_2$ (b) films. Inset in B: SEM image of the $Au-TiO_2$ film (cross sectional view).

used as a photoanode when it is combined with I^- as an electron donor. However, the open-circuit photovoltage was 0.125 V and IPCE was about 1%. To improve these characteristics, we have to optimize the donor and its concentration. The use of the I^-/I_3^- couple is also disadvantageous from the viewpoint of stability because of its corrosive property toward metals including gold. $[Fe(CN)_6]^{4-}$, I^-, Fe^{2+}, ferrocenecarboxylic acid, Br^-, 1,1′-ferrocenedicarboxylic acid, and Cl^- were examined as electron donors. The apparent formal potential $E^{0'}_{app}$ of each donor was evaluated by cyclic voltammetry as the average of anodic and cathodic peak potentials obtained at a platinum electrode [$E^{0'}_{app} = (E_{p,a} + E_{p,c})/2$].

Photoelectrochemical measurements were performed with a cell with a $Au-TiO_2$ photoanode, a platinum wire cathode, and a N_2-saturated acetonitrile and ethylene glycol (v/v 60/40) solution containing 0.1 M lithium nitrate and 0.1 M donor. The dependencies of open-circuit photovoltage (V_{oc}) and short-circuit photocurrent density (J_{sc}) on the apparent formal potential of different donors are plotted in Figure 3. The open-circuit photovoltage increased linearly as the apparent formal potential shifted positively and then became almost constant. The increase is explained in terms of a simple positive shift in the platinum counter electrode potential with the apparent formal potential. The saturation might be due to suppression of photopotential with decelerated electron transfer from the donor to the hole in the gold particle and accelerated back electron transfer from the gold or TiO_2 conduction band to the oxidized donor. In any event, the maximum photovoltage of the present cell is about 0.75 V.

The kinetics is more clearly reflected by the dependence of the short-circuit photocurrents on the redox potential of the donor/acceptor (acceptor = oxidized donor) couple (Figure 3B). It is obvious that there is an optimum potential for the donor/acceptor redox couple (i.e., electron mediator). The potential should be more negative than that of the hole on the gold nanoparticle; otherwise the donor (reduced mediator) cannot give electrons to the nanoparticles. On the other hand, the potential should be more positive than that of the TiO_2 conduction band; otherwise the acceptor (oxidized mediator) cannot receive electrons from the gold nanoparticles via TiO_2 and the counter electrode. Among the donors examined, Fe^{2+} is the best one since it leads to the largest photocurrent (46 μA cm^{-2}) and an almost optimum photovoltage (0.68 V). It is possible that some ligands coordinate to $Fe^{2+/3+}$ and the complex provides the optimal performances.

To fabricate the cell with better performance, the concentration ratio of Fe^{2+} to Fe^{3+} and the proportion between acetonitrile and ethylene glycol in solvent were optimized. When $FeCl_2$ and $FeCl_3$ concentrations were 0.1 and 0.05 M, respectively, the highest photocurrent and total energy conversion efficiency were obtained. The Nernstian potential was measured at a gold electrode in the electrolyte used and found to be 0.46 $\pm$ 0.02 V, which is almost the same as the theoretical value of 0.46 V. The optimal composition of the solvent was 60 vol % acetonitrile and 40 vol % ethylene glycol. In addition, the photocurrent changes obtained after consecutive measurements in this solution for more than 3 days did not exceed 8%. The photoelectrochemical performance exhibited here was stable and reproducible.

Optimized Photovoltaic Cell Performance. Action spectra of the optimized photovoltaic cell were compared with the absorption spectrum of the gold nanoparticles incorporated into the TiO_2 film (Figure 4, solid curves). The photopotential action spectra of the $Au-TiO_2$ film obtained in N_2-saturated acetonitrile and ethylene glycol (v/v 60/40) solution containing 0.1 M lithium nitrate are depicted in Figure 4A. A remarkable negative shift of the open-circuit potential was observed at the $Au-TiO_2$ film under monochromatic visible light illumination, while no obvious change was obtained at a TiO_2 film as reported in our previous work[19] because TiO_2 absorbs only UV light. The maximum potential response ($\sim$170 mV) was observed exactly at the absorption peak wavelength. The action spectrum for potential changes was in good agreement with the absorption spectrum of gold nanoparticles incorporated into the TiO_2 film; the negative potential shift under visible light irradiation was ascribed to the surface plasmon absorption of the gold nanoparticles.

The short-circuit currents were also obtained at the $Au-TiO_2$ film under visible light illumination in the presence of the redox couple $FeCl_2/FeCl_3$. An increased anodic phototcurrent was observed as the visible light was turned on and the current almost returned to the background when irradiation was ceased. IPCE was evaluated from the short-circuit photocurrent as shown in Figure 4B. The photocurrent action spectrum coincided very well with the absorption spectrum of gold nanoparticles in the

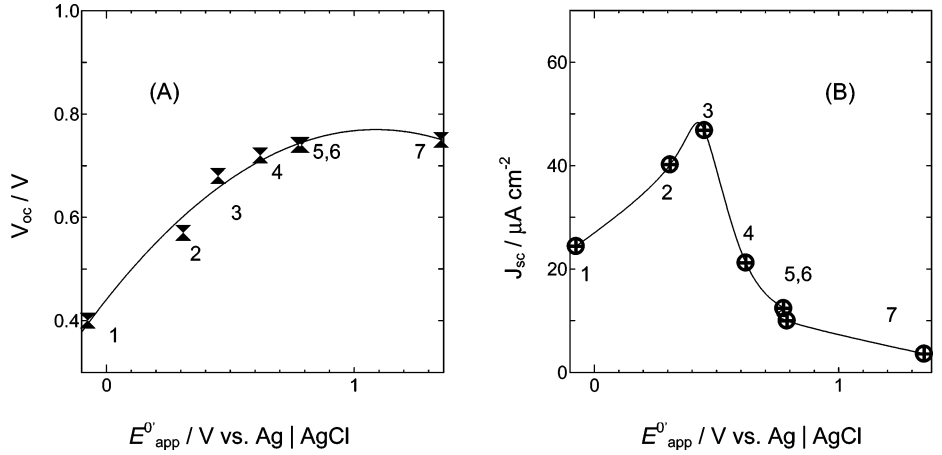

Figure 3. Plots of (A) open-circuit photovoltages and (B) short-circuit photocurrent densities vs apparent formal potential of different donors (1, $[Fe(CN)_6]^{4-}$; 2, I^-; 3, Fe^{2+}; 4, ferrocenecarboxylic acid; 5, Br^-; 6, 1,1′-ferrocenedicarboxylic acid; 7, Cl^-) for the cell with the Au−TiO_2 photoanode, a Pt cathode, and acetonitrile and ethylene glycol (v/v 60/40) containing 0.1 M $LiNO_3$ and 0.1 M donor. The anode was irradiated with a Xe lamp with a UV-cutoff filter (10 mW cm^{-2}).

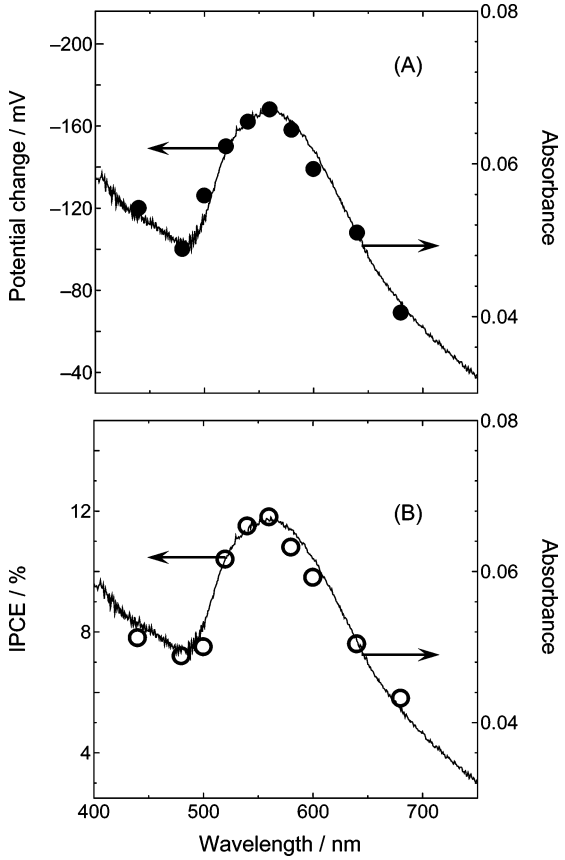

Figure 4. Action spectra for changes in open-circuit potential (A) and IPCE (B) of the Au−TiO_2 film in a N_2-saturated acetonitrile and ethylene glycol (v/v: 60/40) solution containing 0.1 M $LiNO_3$ (and (B) 0.1 M $FeCl_2$ and 0.05 M $FeCl_3$) in response to visible light irradiation (1.36×10^{14} photons cm^{-2} at each wavelength). A conventional cell was employed in the measurements of open-circuit potential with a KCl-saturated Ag|AgCl reference electrode. A two-electrode sandwich cell (thickness of electrolyte, 5 mm) was used in the measurements of IPCE with a Au film cathode.

TiO_2 film and showed the maximum IPCE (∼12%) at around 560 nm. Furthermore, we found that the absorption spectrum of gold nanoparticles obtained after the consecutive photocurrent measurements for over 5000 s had no intrinsic changes compared to that before the measurements. Therefore, it is clear that the photocurrent was attributed not to the irreversible

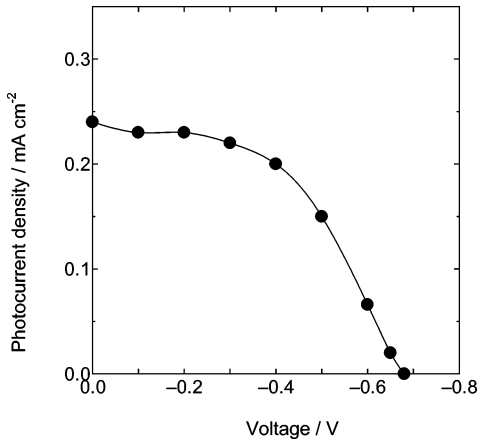

Figure 5. Photocurrent−voltage characteristics of the cell with the Au−TiO_2 film photoanode, a Au film cathode, and the acetonitrile−ethylene glycol solution containing 0.1 M $LiNO_3$, 0.1 M $FeCl_2$, and 0.05 M $FeCl_3$ under white light illumination (> 420 nm, 10 mW cm^{-2}).

oxidation (e.g., corrosion) of gold, but to the electron transport from the cathode via the $Fe^{2+/3+}$ redox couple. In addition, a TiO_2 film that has been treated with $HAuCl_4$ but not irradiated with UV light was also examined, and no photoresponses were obtained.

The photocurrent−voltage curve for the sandwich-type cell was examined under a Xe lamp (10 mW cm^{-2}) (Figure 5). The fill factor (ff) was 0.50 and total energy conversion efficiency (η) was 1.27%. Since these performances are currently much lower than those of the optimized dye-sensitized solar cell with an inorganic dye with organic ligands,[24] the present system should be optimized further for practical use.

Addition of 0.2 M 4-nitrobenzoic acid to the electrolyte further improved the maximum IPCE to 26%, probably because the adsorbed layer of 4-nitrobenzoic acid on TiO_2 blocks the surface levels and suppresses recombination.[25] Likewise, still there are possibilities to improve the performances. In the meantime, since the spectrum given in Figure 4 is a differential spectrum, from which the spectrum of TiO_2 has been subtracted, the absorbance does not reflect the overall photon absorption

(24) Nazeeruddin, M. K.; et al. *J. Am. Chem. Soc.* **2001**, *123*, 1613−1624.
(25) Yang, M.; Thompson, D. W.; Meyer, G. J. *Inorg. Chem.* **2000**, *39*, 3738−3739.

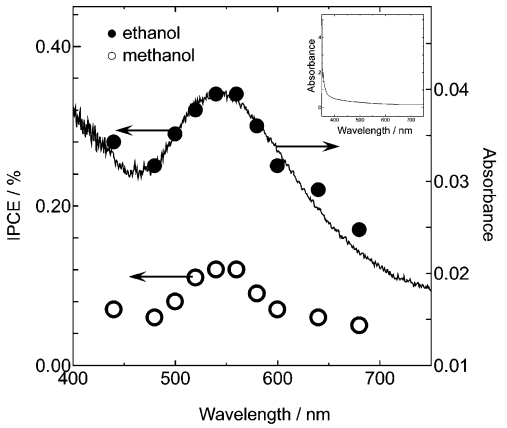

Figure 6. Action spectra for IPCE of the Au−TiO_2 film in the N_2-saturated acetonitrile−ethylene glycol solution containing 0.1 M $LiNO_3$ and 0.5 M ethanol (or methanol) in response to visible light illumination (1.36×10^{14} photons cm^{-2} at each wavelength). Absorption spectrum of an unmodified TiO_2 film is given in the inset.

for all the gold nanoparticles in the film. The present TiO_2 film scatters light significantly (Figure 2A-a), and the gold nanoparticles inside absorb scattered photons also, although the absorption of the scattered light is not reflected by the absorbance in the differential spectrum. The absorption of the scattered light is well known to improve IPCE, so that opaque TiO_2 films are preferably used for dye-sensitized solar cells. From the spectrum of our Au−TiO_2 film (Figure 2A-b), 60% of the light could be absorbed by gold nanoparticles at the most. Therefore, the IPCE value of 26% is a possible value.

Applicability to a Visible-Light-Sensitive Photocatalyst and a Photovoltaic Fuel Cell. The photocatalytic ability of the Au−TiO_2 for oxidation of alcohols was examined. Figure 6 shows the photocurrent action spectra of the Au−TiO_2 film in the N_2-saturated electrolyte with the addition of 0.5 M ethanol or 0.5 M methanol under visible light illumination. An anodic photocurrent was yielded at the Au−TiO_2 film as the visible light was irradiated, while the current was observed neither at a TiO_2 film under visible light irradiation nor at the Au−TiO_2 film when the light was turned off. Furthermore, the photocurrent action spectra closely fitted the absorption spectrum of the gold nanoparticles incorporated into the TiO_2 film, which shows the surface plasmon adsorption characteristic of gold nanoparticles. It indicates that both ethanol and methanol can be an electron donor for the Au−TiO_2 photoanode, although the IPCE values were about 0.30% and 0.12%, respectively. Incidentally, it is known that electrocatalytic activity for alcohol oxidation depends strongly on the electrode material.[26] The low efficiencies may be due to poor catalytic ability of gold for alcohol oxidation.[27] The efficiency could be improved by optimizing temperature, pH, and solvents or modification of the Au−TiO_2 film with an appropriate catalyst such as platinum.

The photoelectrochemical oxidation of alcohols was further studied. We first examined the photocatalytic oxidation of ethanol. The probable products of ethanol oxidation include acetaldehyde (CH_3CHO), ethyl acetate ($CH_3COOCH_2CH_3$), and acetic acid (CH_3COOH). We measured short-circuit photocurrents in the presence of CH_3CHO, $CH_3COOCH_2CH_3$, and CH_3COOH at the Au−TiO_2 film in the N_2-saturated electrolyte under white light irradiation (>420 nm, 10 mW cm^{-2}). A photoanodic current was observed in the presence of either CH_3CHO or $CH_3COOCH_2CH_3$, while no obvious photocurrent was obtained in the presence of CH_3COOH. Thus, we infer that the final product would be CH_3COOH.

We also checked formaldehyde (HCHO), 2-methoxyethanol (CH_3OCH_2OH), formaldehyde dimethyl acetal ($CH_3OCH_2OCH_3$), ethyle formate ($HCOOCH_3$), and formic acid (HCOOH) as probable products of photocatalytic oxidation of methanol and concluded that the final product could be HCOOH.

In addition, O_2 was bubbled into the electrolyte containing 0.5 M ethanol. As a result, the anodic photocurrent gradually decreased and reached about 10% of the maximum photocurrent in 30 min. It is clear that O_2, a typical electron acceptor, takes photoexcited electrons from the gold nanoparticles directly or via TiO_2 (described later) so as to interfere with the photoanodic current. Actually, H_2O_2 was detected in the solution by using enzyme peroxidase and 2,2′-azinobis(3-ethylbenzothiazoline-6-sulforic acid). This result supports the reduction of oxygen, since H_2O_2 is one of the possible products of oxygen reduction.

These results indicate that the present Au−TiO_2 system is potentially applicable to a visible-light-sensitive photocatalyst that oxidizes ethanol and methanol at the expense of O_2 reduction. This is an exactly different phenomenon from that reported previously for photocatalysis at semiconductor−metal nanocomposites, in which metal nanoparticles have been used as a sink for charge carriers photoexcited in the semiconductor.[16] In addition, the present system is also potentially applicable to a photovoltaic fuel cell, in which photocurrents can be obtained with an alcohol and O_2. Although IPCE of the recently reported enzyme-based photovoltaic fuel cell (about 35%)[28] is much higher than that of our system, potential advantages of our system might include stability (the lifetime is not limited by enzyme) and wide adaptabilities to temperature, pH, and solvents.

Mechanisms of the Charge Separation. The most important point in the mechanism of the present system is how the charges are separated. First, to examine the electron transfer from the gold nanoparticles to TiO_2, we carried out spectroscopic measurements of the irradiated TiO_2. It is known that TiO_2 is colored when a potential more negative than its flatband potential is applied.[28] Thus, if TiO_2 is colored under irradiation of the open-circuited Au−TiO_2 in the presence of an irreversible donor, it suggests that electrons are transferred from the irradiated gold to TiO_2 conduction band.

The absorbance changes at 680 nm were measured at a Au−TiO_2 film in a N_2-saturated electrolyte solution containing 0.5 M ethanol as an irreversible donor under white light (>500 nm) irradiation (Figure 7). The absorbance at 680 nm of the Au−TiO_2 film gradually increased under white light and decreased quickly when O_2 was bubbled. In contrast, absorbance was completely constant when TiO_2 without Au was irradiated under the same conditions. The absorption band observed for Au−TiO_2 was quite broad over the visible range, indicating that the spectrum change was not due to the gold nanoparticles, but TiO_2.[29] Actually, a similar spectrum change was observed when

(26) Zhou, W. J.; et al. *J. Power Sources* **2004**, *126*, 16−22.
(27) Tremiliosi-Filho, G.; Gonzalez, E. R.; Motheo, A. J.; Belgsir, E. M.; Léger, J.-M.; Lamy, C. *J. Electroanal. Chem.* **1998**, *444*, 31−39.
(28) Garza, L.; Jeong, G.; Liddell, P.; Sotomura T.; Moore, T.; Moore, A.; Gust, D. *J. Phys. Chem. B* **2003**, *107*, 10252−10260.
(29) Boschloo, G.; Fitzmaurice, D. *J. Phys. Chem. B* **1999**, *103*, 7860−7868.

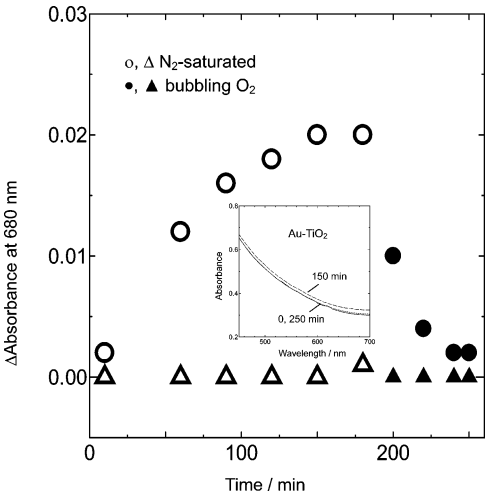

Figure 7. Changes in absorbance at 680 nm for the open-circuited Au−TiO_2 film (circles) and TiO_2 films (triangles) in a N_2-saturated acetonitrile−ethylene glycol solution containing 0.1 M $LiNO_3$ and 0.5 M ethanol under 10 mW cm^{-2} white light illumination (>500 nm) before (open circles and triangles) and after (filled circles and triangles) O_2 bubbling. Inset: Absorption spectra of the Au−TiO_2 film at 0, 150, and 250 min.

a potential negative of −0.9 V was applied to the ITO electrode coated with the Ag−TiO_2. Thus, it was verified that the photoexcited electrons at the gold particles are injected into the TiO_2 conduction band (Figure 1), and the injected electrons can be transferred to O_2 in turn. Since a Schottky barrier is formed at gold/TiO_2 junctions due to the large work function of gold[30] (Figure 1), observation of the electron transfer from the photoexcited gold to nonexcited TiO_2 is not surprising.

Next, the electron transfer from a donor to the gold particles was examined. Figure 8 shows the spectrum changes for the Au−TiO_2 film in the N_2-saturated electrolyte without donor under 10 mW cm^{-2} white light (>500 nm) irradiation. The visible light generated the photoexcited state of the gold nanoparticles due to the surface plasmon resonance, and the excited electrons were injected into the TiO_2 bulk. Hence, the gold nanoparticles lost electrons, resulting in a decrease of their absorbance, as shown by curve b in Figure 8. It is probable that the electrons and holes are spatially separated rapidly and electrostatically stabilized by counterions in the electrolyte. In the absence of an electron donor, the coloring of TiO_2 is negligible because the amount of injected electrons is so small. The injected electrons are gradually transferred back to the oxidized gold nanoparticles. However, with the addition of ethanol, an irreversible electron donor, the intact, photoresponsive gold nanoparticles are rapidly regenerated (curve c in Figure 8); electrons are transferred from the donor to the gold nanoparticles.

(30) Tang, J.; White, M.; Stucky, G. D.; McFarland, E. W. *Electrochem. Commun.* **2003**, *5*, 497−501.

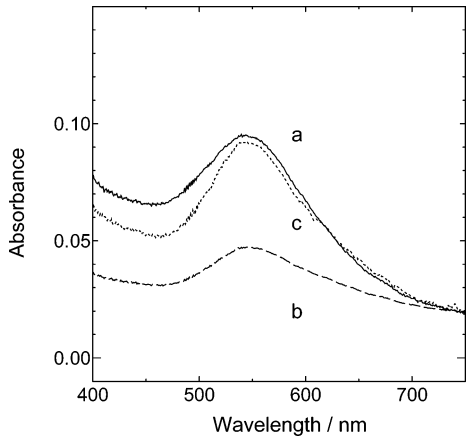

Figure 8. Absorption spectra of the Au−TiO_2 film in the N_2-saturated electrolyte (the spectrum of TiO_2 has been subtracted). The open-circuited Au−TiO_2 film (a) was irradiated with white light (10 mW cm^{-2}, >500 nm) for 30 min (b), and then ethanol (0.5 M) was added to the electrolyte (c).

Accordingly, the mechanism of the plasmon-induced charge separation was clarified as follows: visible light generates the photoexcited state of the gold nanoparticles based on the surface plasmon resonance. Then the photoexcited electrons are injected into the TiO_2 bulk. Simultaneously, the oxidized gold nanoparticles take electrons from a donor in the solution (Figure 1).

Conclusions

Charge separation at the plasmon-excited gold nanoparticles incorporated in TiO_2 was verified. It was found that the charge separation is accomplished by electron transfer from the excited gold particles to TiO_2 and that from a donor to the gold particle. As a low-cost photovoltaic cell, its incident photon to current conversion efficiency (IPCE) is 12% with the $Fe^{2+/3+}$ redox mediator. In addition, the Au−TiO_2 was newly found to function as a new class of visible-light-sensitive photocatalysts that oxidizes ethanol and methanol and reduces oxygen. Thus, a photovoltaic fuel cell is now one of its potential applications.

Acknowledgment. This work was supported in part by a Grant-in-Aid for Scientific Research on Priority Areas (417) from the Ministry of Education, Culture, Sports, Science and Technology of Japan. Y.T. thanks the Japan Society for the Promotion of Science (JSPS) for the postdoctoral fellowship.

Supporting Information Available: Complete refs 24 and 26. This material is available free of charge via the Internet at http://pubs.acs.org.

JA042192U